exo-nido-Monothio- and *exo-nido*-Monophosphinorhodacarboranes: Synthesis, Reactivity, and Catalytic Properties in Alkene Hydrogenation†

Clara Viñas,‡ Miguel A. Flores,‡ Rosario Núñez,‡ Francesc Teixidor,*,‡ Raikko Kivekäs,§ and Reijo Sillanpää||

Institut de Ciència de Materials de Barcelona, CSIC, Campus de Bellaterra, Cerdanyola, 08193 Barcelona, Spain, Inorganic Chemistry Laboratory, Box 55, University of Helsinki, FIN-00014 Helsinki, Finland, and Department of Chemistry, University of Turku, FIN-20500 Turku, Finland

Received November 17, 1997

Reaction of Cs[7-SR-8-R′-7,8-$C_2B_9H_{10}$] (R = Ph, R′ = Me; R, R′ = Ph; R = Et, R′ = Me) with [RhCl(PPh_3)$_3$] in toluene−ethanol (8:1) affords [Rh(7-SR-8-R′-7,8-$C_2B_9H_{10}$)(PPh_3)$_2$]. Reaction of tetraalkylammonium salts of [7-PR_2-8-R′-7,8-$C_2B_9H_{10}$]$^-$ (R = Ph, R′ = H; R = Ph, R′ = Me; R, R′ = Ph; R = Et, R′ = Me; R = Et, R′ = Ph; R = ^{i}Pr, R′ = Me) with [RhCl(PPh_3)$_3$] in ethanol affords [Rh(7-PR_2-8-R′-7,8-$C_2B_9H_{10}$)(PPh_3)$_2$]. The structure of [Rh(7-PPh_2-8-H-7,8-$C_2B_9H_{10}$)(PPh_3)$_2$] has been determined by crystallographic studies. Rh(I) has a normal four-coordinated square-planar geometry. The carborane ligand is bonded to the metal by means of a P−Rh and a B(11)−H−Rh bond. Two PPh_3 ligands fulfill the coordination sphere of the metal. The spectroscopic data indicate analogous structures for the rest of the complexes. [Rh(7-SPh-8-Me-7,8-$C_2B_9H_{10}$)(PPh_3)$_2$] reacts with L = PPh_3, $PMePh_2$, and PEt_3 to give the salts [RhL_4][7-SPh-8-Me-7,8-$C_2B_9H_{10}$]. [Rh(7-PPh_2-8-H-7,8-$C_2B_9H_{10}$)(PPh_3)$_2$] does not react with PPh_3, but it does react with L = $PMePh_2$, PMe_2Ph, and PEt_3 to give different substitution products depending on the complex:phosphine ratio: [Rh(7-PPh_2-8-H-7,8-$C_2B_9H_{10}$)(PPh_3)L] at the ratio 1:1, [Rh(7-PPh_2-8-H-7,8-$C_2B_9H_{10}$)L_2] at the ratio 1:2, and [RhL_4][7-PPh_2-8-H-7,8-$C_2B_9H_{10}$] at ratios higher than 1:3. Both the thioether and the phosphino families catalyze the hydrogenation of 1-hexene to *n*-hexane. The thioether family is an active catalyst at P = 1 bar and T = 25 °C, whereas the phosphino family requires higher temperatures and pressures. The hydrogenation of 2-hexenes proceeds much more slowly than for 1-hexene. Both catalytic systems are recoverable upon completion of reaction. [Rh(7-PPh_2-8-H-7,8-$C_2B_9H_{10}$)(PPh_3)$_2$] and [Rh(7-PPh_2-8-Me-7,8-$C_2B_9H_{10}$)(PPh_3)$_2$] catalyze the hydrogenation of the antibiotic precursor methacycline to doxycycline with high yield and very high diastereoselectivity (ca. 100%) for the pharmacologically important molecule. The other possible isomer *epi*-doxycycline was not observed in any case.

Introduction

The use of rhodacarboranes as homogeneous catalysts for the hydrogenation and isomerization of alkenes was first reported[1,2] by Hawthorne and co-workers in 1974. Later, the formal 18-electron Rh(III) *closo*-rhodacarborane clusters were shown to be in equilibrium with variable amounts of an *exo-nido* 16-electron Rh(I) tautomer,[3−5] in which the [Rh(PPh_3)$_2$]$^+$ moiety is bonded to the carborane cage through a pair of B−H−Rh three-center, two-electron bonds. A thorough mechanistic study[6−8] attributed the catalytic activity to the formation of B−Rh^{III}−H species by the oxidative addition of terminal B−H bonds to Rh(I) centers in *exo-nido*-rhodacarborane derivatives.

We have recently reported[9] the synthesis of the new *exo-nido*-rhodacarborane complex [Rh(7-SPh-8-Me-7,8-$C_2B_9H_{10}$)(PPh_3)$_2$], which has exhibited very high cata-

† On the occasion of the 80th birthday of our teacher Prof. Heribert Barrera i Costa, in recognition of his outstanding personal and professional merits.

‡ Institut de Ciència de Materials de Barcelona, CSIC.

§ University of Helsinki.

|| University of Turku.

(1) Paxson, T. E.; Hawthorne, M. F. *J. Am. Chem. Soc.* **1974**, *96*, 4674−4677.

(2) Baker, R. T.; Delaney, M. S.; King, R. E.; Knobler, C. B.; Long, J. A.; Marder, T. B.; Paxson, T. E.; Teller, R. G.; Hawthorne. M. F. *J. Am. Chem. Soc.* **1984**, *106*, 2965−2978.

(3) Long, J. A.; Marder, T. B.; Behnken, P. E.; Hawthorne. M. F. *J. Am. Chem. Soc.* **1984**, *106*, 2979−2989.

(4) Knobler, C. B.; Marder, T. B.; Mizusawa, E. A.; Teller, R. G.; Long, J. A.; Behnken, P. E.; Hawthorne, M. F. *J. Am. Chem. Soc.* **1984**, *106*, 2990−3004.

(5) Long, J. A.; Marder, T. B.; Hawthorne, M. F. *J. Am. Chem. Soc.* **1984**, *106*, 3004−3010.

(6) Behnken, P. E.; Belmont, J. A.; Busby, D. C.; Delaney, M. S.; King, R. E.; Kreimendahl, C. W.; Marder, T. B.; Wilczynski, J. J.; Hawthorne, M. F. *J. Am. Chem. Soc.* **1984**, *106*, 3011−3025.

(7) Behnken, P. E.; Busby, D. C.; Delaney, M. S.; King, R. E.; Kreimendahl, C. W.; Marder, T. B.; Wilczynski, J. J.; Hawthorne, M. F. *J. Am. Chem. Soc.* **1984**, *106*, 7444−7450.

(8) Belmont, J. A.; Soto, J.; King, R. E.; Donaldson, A. J.; Hewes, J. D.; Hawthorne, M. F. *J. Am. Chem. Soc.* **1989**, *111*, 7475−7486.

(9) Teixidor, F. T.; Flores, M. A.; Viñas, C.; Kivekäs, R.; Sillanpää, R. *Angew. Chem., Int. Ed. Engl.* **1996**, *35*, 2251−2253.

S0276-7333(97)01019-4 CCC: $15.00
Publication on Web 05/08/1998

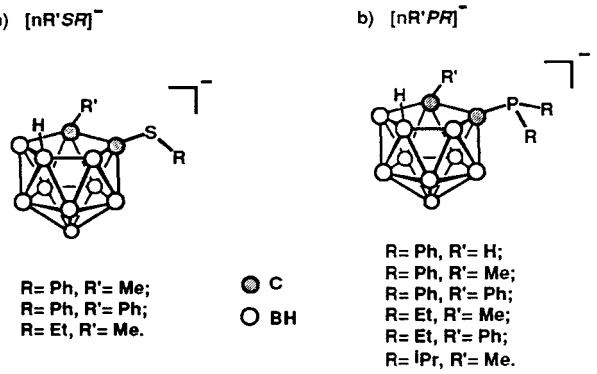

Figure 1. Schematic drawing of *nido*-monothio- and *nido*-monophosphinocarborane anions along with their abbreviations.

lytic activity in the hydrogenation of 1-hexene. These results prompted us to start a systematic search for rhodium complexes of 7,8-C_2B_9 clusters incorporating one electron-rich element bonded to an open-face carbon atom and study their possible implications in catalysis. In this paper, the preparation of monothio- and monophosphinorhodacarborane complexes is described and the spectroscopic, chemical, and catalytic properties are reported. Throughout the text the ligand [7-SR-8-R′-7,8-$C_2B_9H_{10}$]$^-$ will be abbreviated as [nR′*SR*]$^-$, where n represents the moiety [7,8-$C_2B_9H_{10}$]$^-$ and R and R′ the organic radicals connected to S and C(8), respectively. Similarly, the ligand [7-PR_2-8-R′-7,8-$C_2B_9H_{10}$]$^-$ will be abbreviated as [nR′*PR*]$^-$ (see Figure 1). No attempt to resolve the *nido*-carborane ligands into their enantiomers has been made in this work, and we have used the racemic ligands consistently.

Results and Discussion

Synthesis and Characterization of *exo-nido*-Monothiorhodacarboranes. Preliminary attempts to prepare (monothiocarborane)rhodium complexes by refluxing [NMe_4][nMe*SPh*] and [RhCl(PPh_3)$_3$] in ethanol for variable periods of time (2−24 h) were unsuccessful, yielding the starting rhodium complex and variable amounts of [RhCl(CO)(PPh_3)$_2$], produced by decarbonylation of the solvent. The use of butanol at reflux for several hours produced [RhCl(CO)(PPh_3)$_2$] as the main product. Treatment of [RhCl(PPh_3)$_3$] with an ethanolic solution of $AgClO_4$ and subsequent reaction with [NMe_4]-[nMe*SPh*] were also unsuccessful. An alternative procedure[3] based on the synthesis of the *exo-nido*-rhodacarboranes of formula [Rh(7-R-8-R′-7,8-$C_2B_9H_{10}$)(PPh_3)$_2$] (R, R′ = alkyl, aryl) was then attempted. The method consists of using the cesium salt of the carborane anion to precipitate the chloride ligand as CsCl. The reaction of the cesium salt of ligands [nR′*SR*]$^-$ with [RhCl(PPh_3)$_3$] in a toluene−ethanol (8:1) mixture at room temperature yielded the complexes [Rh(nMe*SPh*)(PPh_3)$_2$], [Rh(nPh*SPh*)(PPh_3)$_2$], and [Rh(nMe*SEt*)(PPh_3)$_2$] in 82−91% yield. The spectroscopic data and elemental analyses were consistent with (*exo-nido*-monothiocarborane)rhodium complexes containing two triphenylphosphine ligands per molecule. The IR spectra displayed a band near 2100 cm^{-1}, and the ^{1}H NMR spectra showed broad resonances in the B−H−B bridge zone and at ca. −4.5 ppm, the latter being characteristic

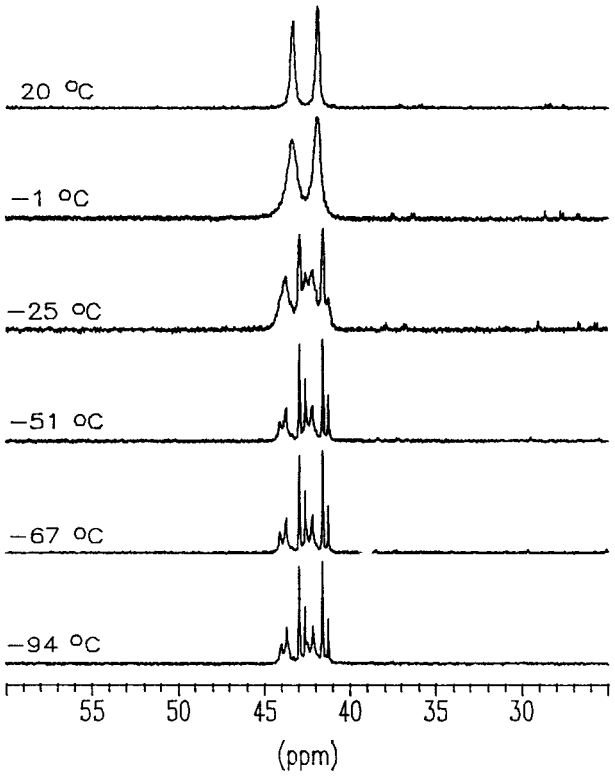

Figure 2. Variable-temperature ^{31}P{^{1}H} NMR spectra of [Rh(nMe*SEt*)(PPh_3)$_2$] in CD_2Cl_2 (the spectra follow an AB pattern).

of B−H−Rh interactions. The ^{31}P{^{1}H} NMR spectra of the complexes revealed the existence of a dynamic process. For [Rh(nMe*SPh*)(PPh_3)$_2$] and [Rh(nMe*SEt*)-(PPh_3)$_2$], the spectra showed broad doublets at 42.8 ppm (^1J(Rh,P) = 176 Hz) and 42.6 ppm (^1J(Rh,P) = 180 Hz), respectively, while that of [Rh(nPh*SPh*)(PPh_3)$_2$] presented only a broad resonance centered at 42.7 ppm. These broad resonances could be resolved at low temperatures to give two doublets of doublets characteristic of two triphenylphosphine ligands of a [Rh(PPh_3)$_2$]$^+$ fragment in relative cis positions (Figures 2 and 3). The resonances at lower field presented higher Rh−P coupling constants (^1J(Rh,P) = 187−193 Hz) than those situated at upper field (^1J(Rh,P) = 158−165 Hz). This higher value is characteristic of a phosphorus atom bound to rhodium having a weakly coordinating ligand in a relative trans position[10] and most probably belongs to a PPh_3 ligand trans to a B−H group. Besides, the lower field resonance was typically broader than the one situated at upper field and we attribute this broadness to coupling to the boron atom belonging to the *trans*-B−H group. On the other hand, the low-temperature ^{1}H{^{11}B} NMR spectra of the complexes showed a small upper field shift of B−H−B and B−H−Rh resonances. An X-ray diffraction study[9] of [Rh(nMe*SPh*)(PPh_3)$_2$] confirmed the stereochemistry deduced from the spectroscopic data and revealed that the carborane cage chelates the metal by means of a S−Rh and a B(11)−H−Rh bond (Figure 4).

The solutions of the three (*exo-nido*-monothiocarborane)rhodium complexes are air-sensitive. Moreover,

(10) Collman, J. P.; Hegedus, L. S.; Norton, J. R.; Finke, R. G. *Principles and Applications of Organotransition Metal Chemistry*; University Science Books: Mill Valley, CA, 1987; p 72.

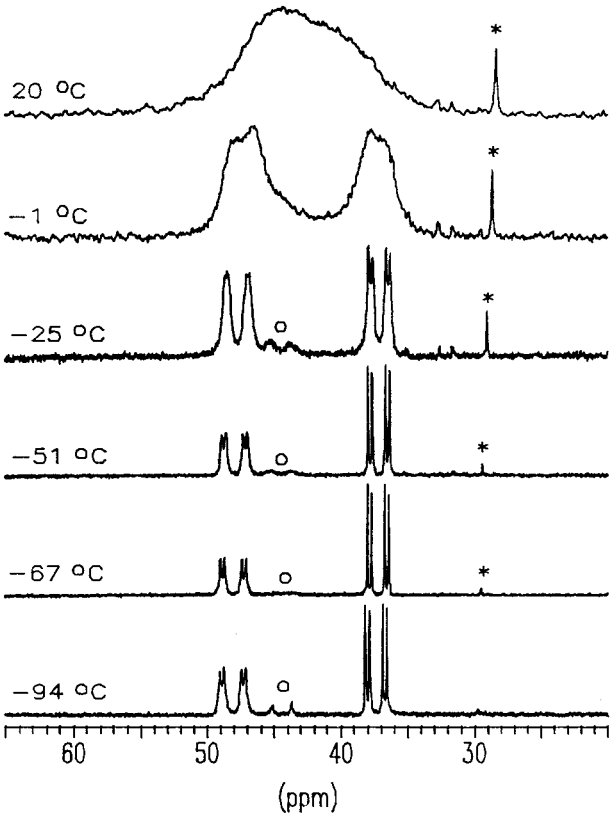

Figure 3. Variable-temperature $^{31}P\{^1H\}$ NMR spectra of $[Rh(nPhSPh)(PPh_3)_2]$ in CD_2Cl_2: (*) $OPPh_3$; (○) trace impurity.

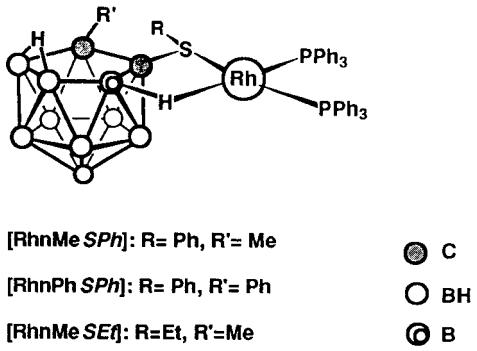

[RhnMe *SPh*]: R= Ph, R'= Me
[RhnPh *SPh*]: R= Ph, R'= Ph
[RhnMe *SEt*]: R=Et, R'=Me

C
BH
B

Figure 4. Schematic drawing of $[Rh(nR'SR)(PPh_3)_2]$ complexes.

in the solid state, $[Rh(nMeSPh)(PPh_3)_2]$ and $[Rh(nMeSEt)(PPh_3)_2]$ showed evidence of decomposition after several months exposed to air, and for that reason they are best stored under N_2. This degradation process is much faster for $[Rh(nPhSPh)(PPh_3)_2]$, whose pale orange color gradually faded to dark orange within days. The IR spectrum of the solid showed a decrease of the B−H band intensity while new broad bands near 3200, 1400, and 1200 cm^{-1}, characteristic of borates, appeared. The ^{11}B NMR spectrum revealed a new singlet at 20.5 ppm which confirmed the formation of $B(OR)_3$. Also, the $^{31}P\{^1H\}$ NMR spectrum displayed one single signal at 27.7 ppm which corresponds to $OPPh_3$ species. These data indicate that the atmospheric O_2 irreversibly reacts with $[Rh(nPhSPh)(PPh_3)_2]$, producing degradation of the cluster. These data also account for the difference found between the experimental and expected elemental analyses of the complex.[11] The same applies for most of the monophosphinorhodacarboranes indicated next. The addition of 0.1−0.2 B_2O_3 per formula unit produces perfect agreement between calculated and found analyses. This implies a certain degree of decomposition of the complexes upon purification which we have not been able to solve fully.

Synthesis and Characterization of *exo-nido*-Monophosphinorhodacarboranes. The tetraalkylammonium salts of *nido* ligands $[nR'PR]^-$ (Figure 1) reacted with $[RhCl(PPh_3)_3]$ in refluxing ethanol to yield orange solids with the stoichiometry $[Rh(nR'PR)(PPh_3)_2]$. Thus, there was no need to use the cesium salts of ligands $[nR'PR]^-$ to obtain the respective rhodium complexes. These results prove that, in contrast to the case for the *nido*-monothiocarborane ligands $[nRSR]^-$, the analogous phosphorus compounds $[nR'PR]^-$ are able to remove the chloride ligand from the coordination sphere of the rhodium center. Besides, this indicates a stronger coordinating ability of *nido*-monophosphinocarborane ligands compared to that of the sulfur analogues. This behavior was observed before in the reaction of the tetramethylammonium salts of ligands $[nMePPh]^-$ and $[nMeSPh]^-$ with the complex $[RuCl_2(Me_2SO)_4]$.[12] While $[nMePPh]^-$ was able to remove all ligands from the coordination sphere of the ruthenium center to produce $[Ru(nMePPh)_2]$, only free ligand was recovered when $[nMeSPh]^-$ was used.

The IR spectra of $[Rh(nR'PR)(PPh_3)_2]$ complexes showed one band near 2000 cm^{-1} which could be assigned to B−H−Rh interactions. The ^1H NMR spectra showed broad resonances in the B−H−B bridge zone and unresolved quartets between −3.68 and −5.60 ppm (B−H−Rh, $^1J(B,H) = 86-96$ Hz). The B−H−Rh resonances appeared in the $^1H\{^{11}B\}$ NMR spectra as multiplets, probably arising from coupling to both rhodium and phosphorus. The $^{31}P\{^1H\}$ NMR spectra (Table 1 and Figure 5) displayed three sets of resonances indicating three different phosphorus atoms in the molecule. As in the (monothiocarborane)rhodium complexes, the higher coupling constant and broadness of the lowest field resonances (P_a) indicate that this phosphorus is in a trans position relative to the B−H group coordinated to rhodium. When the temperature was lowered to −94 °C, the P_a resonance was resolved, giving a broad doublet of triplets ($^1J(Rh,P) = 197-198$ Hz, $^{cis}J(P,P) = 35-40$ Hz) (Figure 6). Since no other new signals appeared in the low-temperature $^{31}P\{^1H\}$ NMR spectra, this resolution is attributed to thermal decoupling of the boron atoms.[13] On the other hand, the highest field set of resonances (P_c in Figure 5) spanned a relatively wide zone (2.31−24.29 ppm), depending on the R groups attached to the $C_{cage}-PR_2$ moiety, whereas the other set (P_b) appeared in a much narrower range (27.43−30.20 ppm). For this reason, the P_c set is assigned to the $C_{cage}-PR_2$ group and the P_b set is assigned to the PPh_3 in a relative trans position. Thus, the spectroscopic data

(11) The experimental analyses give an atomic ratio of C:H = 1:1, which is in agreement with the ratio of $C_{50}H_{50}B_9P_2SRh$ (the sulfur analysis has not been considered, since it usually gives lower values than expected). However, the percent values are lower than expected. The formation of $B(OR)_3$ during the analytical manipulation would account for those observations.

(12) Teixidor, F.; Viñas, C.; Nuñez, R.; Flores, M. A.; Kivekäs, R.; Sillanpää, R. *Organometallics* **1995**, *14*, 3952.

(13) Beall, H.; Bushweller, C. H. *Chem. Rev.* **1973**, *73*, 465 and references therein.

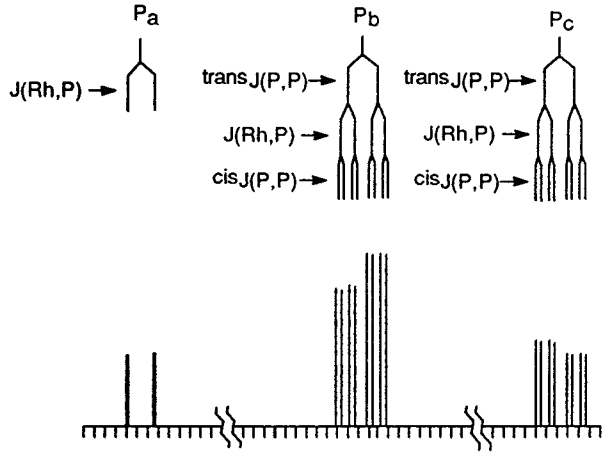

Figure 5. Schematic representation of the $^{31}P\{^1H\}$ NMR spectrum of [Rh(nR′*PR*)$(PPh_3)_2$] complexes.

Table 1. $^{31}P\{^1H\}$ NMR Spectroscopic Data for [Rh(nR′*PR*)$(PPh_3)_2$] Complexes

δ, ppm	mult	^1J(Rh,P), Hz	$^{trans}J$(P,P), Hz	^{cis}J(P,P), Hz	assignt
		(Rh(nH*PPh*)$(PPh_3)_2$]			
2.31	ddd	169	282	43	P_c
27.43	ddd	159	282	31	P_b
48.06	br d	199			P_a
		(Rh(nMe*PPh*)$(PPh_3)_2$]			
4.55	ddd	124	283	41	P_c
30.20	ddd	128	283	32	P_b
50.10	br d	208			P_a
		(Rh(nPh*PPh*)$(PPh_3)_2$]			
6.64	ddd	123	281	40	P_c
28.28	ddd	128	281	33	P_b
46.51	br d	197			P_a
		(Rh(nMe*PEt*)$(PPh_3)_2$]			
8.25	ddd	123	275	43	P_c
27.96	ddd	124	275	33	P_b
50.89	br d	195			P_a
		(Rh(nPh*PEt*)$(PPh_3)_2$]			
13.57	ddd	119	275	43	P_c
28.50	ddd	125	275	34	P_b
49.46	br d	195			P_a
		(Rh(nMeP^i*Pr*)$(PPh_3)_2$]			
24.29	ddd	123	275	35	P_c
28.29	ddd	119	275	40	P_b
49.17	br d	207			P_c

support a molecular structure similar to that of [Rh(nMe*SPh*)$(PPh_3)_2$]: that is, a square-planar Rh(I) center bonded to a carborane ligand through the phosphorus atom and to a B−H group through one three-center−two-electron B−H−Rh interaction.

An X-ray crystallographic study of [Rh(nH*PPh*)-$(PPh_3)_2$] has confirmed the stereochemistry deduced from the spectroscopic analyses and provided more information about the nature of the interaction of the $[Rh(PPh_3)_2]^+$ fragment and the carborane cage. A simplified drawing of the complex unit is shown in Figure 7. Crystallographic data are provided in Table 2; selected bond lengths and angles are displayed in Table 3. The Rh(I) center has a normal four-coordinated square-planar geometry. The two bonds from the cage to Rh(I) are formed by the phosphorus atom of the diphenylphosphino group and the hydrogen atom (H(11)) bonded to B(11) at the C_2B_3 open face. The two PPh_3 ligands fulfill the coordination plane of the metal. The coordination mode of the carborane ligand is similar to

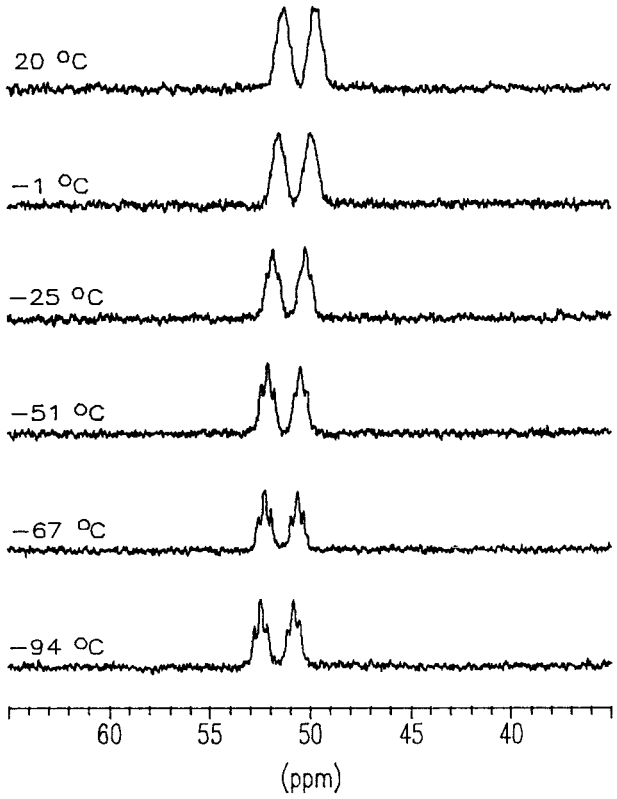

Figure 6. Variable-temperature $^{31}P\{^1H\}$ NMR spectra of [Rh(nMe*PEt*)$(PPh_3)_2$] in CD_2Cl_2 (only the P_a region is presented).

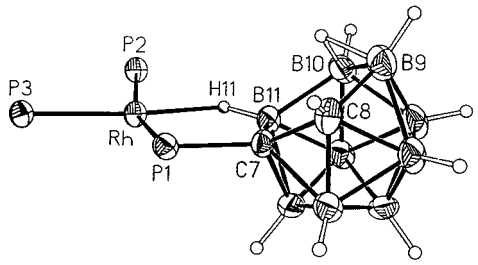

Figure 7. Crystal structure of [Rh(nH*PPh*)$(PPh_3)_2$]. Phenyl rings of PPh_3 ligands are omitted for clarity.

Table 2. Crystallographic Data for [Rh(nH*PPh*)$(PPh_3)_2$]·$3CH_2Cl_2$

chem formula	$C_{50}H_{51}B_9P_3Rh\cdot 3CH_2Cl_2$
fw	199.80
cryst syst	monoclinic
space group	$P2_1/n$ (No. 14)
a	15.987(5) Å
b	18.496(4) Å
c	19.320(4) Å
β	91.22(2)°
V	5712(2) Å^3
Z	4
T	23 °C
λ	0.710 69 Å
ρ	1.395 g cm^{-3}
μ	7.0 cm^{-1}
GOF	1.918
R^a	0.064
$R_w{}^b$	0.068

^{a} $R = \sum||F_o| - |F_c||/\sum|F_o|$. ^{b} $R_w = [\sum w(|F_o| - |F_c|)^2/\sum w|F_o|^2]^{1/2}$.

that for [Rh(nMe*SPh*)$(PPh_3)_2$],[9] the coordination planes being approximately parallel to the C_2B_3 plane. The geometry of these complexes differs markedly from those of [Rh(7-R-8-R′-7,8-$C_2B_9H_{10}$)$(PPh_3)_2$] (R, R′ =

Table 3. Selected Bond Lengths (Å) and Angles (deg) for [Rh(nH*PPh*)(PPh$_3$)$_2$]·3CH$_2$Cl$_2$

Rh−P(1)	2.276(2)	Rh−H(11)	1.81(5)
Rh−P(2)	2.340(2)	P(1)−C(7)	1.808(7)
Rh−P(3)	2.224(2)	C(7)−C(8)	1.551(9)
Rh−B(11)	2.643(8)	B(11)−H(11)	1.12(5)
P(1)−Rh−P(2)	163.14(7)	Rh−P(1)−C(18)	125.4(2)
P(1)−Rh−P(3)	98.29(7)	P(1)−C(7)−B(2)	115.6(5)
P(1)−Rh−H(11)	86(2)	P(1)−C(7)−B(3)	124.6(5)
P(2)−Rh−P(3)	95.93(7)	P(1)−C(7)−C(8)	126.6(5)
P(3)−Rh−H(11)	174(2)	P(1)−C(7)−B(11)	107.0(4)
Rh−P(1)−C(7)	96.7(2)	C(8)−C(7)−B(11)	115.0(5)
Rh−P(1)−C(12)	110.3(2)		

alkyl, aryl) complexes[4] in which the Rh(I) is coordinated to the carborane ligand via H(2) (lower belt) and H(11) (upper belt) atoms. Thus, the coordination planes in [Rh(7-R-8-R′-7,8-$C_2B_9H_{10}$)(PPh$_3$)$_2$] compounds are perpendicular to the C_2B_3 plane.

The stiff boron cage must considerably modify the angles around P(1) and C(7) in order to act as a bidentate ligand. Hence, the angles around P(1) vary from 96.7(2) to 125.4(2)° and for C(7) from 107.0(4) to 126.6(5)°, the smallest angles being for Rh−P(1)−C(7) and P(1)−C(7)−C(8). The Rh−P bonds are dissimilar, with P(3) trans to H(11) forming the shortest bond to the metal (2.224(2) Å) and P(2) trans to the PPh$_2$ group forming the longest Rh−P bond (2.340(2) Å). The differences in the Rh−P bond lengths may be explained in terms of trans influence.

The spectroscopic and structural characterization of the complexes reported in this paper allows several points to be addressed. First, it is interesting to note that no *closo*-monothio- or *closo*-monophosphinorhodacarborane species have been detected either in solution or in the solid state. Earlier, it was observed that the incorporation of organic C_{cage}−alkyl or C_{cage}−aryl groups in [Rh(7-R-8-R′-7,8-$C_2B_9H_{10}$)(PPh$_3$)$_2$] rhodacarborane complexes favored the formation of the *exo-nido* tautomer.[3] However, some C_{cage}-disubstituted complexes still exhibited variable amounts of the *closo* tautomer in solution. Therefore, the presence of the thioether or phosphino moieties appears to provide additional stability to the *exo-nido* species. Second, the NMR spectroscopic data of *exo-nido*-rhodacarboranes of the type [Rh(7-R-8-R′-7,8-$C_2B_9H_{10}$)(PPh$_3$)$_2$] (R, R′ = alkyl, aryl) indicated that the [Rh(PPh$_3$)$_2$]$^+$ fragment did not maintain a static position but most probably migrated around several B−H sites of its polyhedral surface.[3−5] In contrast, the ^{11}B{^{1}H} and ^{31}P{^{1}H} NMR spectra of [Rh(nR′*PR*)(PPh$_3$)$_2$] are sharp and are resolved at ambient temperatures, indicating the presence of only one *exo-nido* isomer in solution. Also, the dynamic process observed in the ^{31}P{^{1}H} NMR spectra of [Rh(nR′*SR*)(PPh$_3$)$_2$] complexes appears to be due to rapid rotation of PPh$_3$ ligands on the NMR time scale rather than migration of the [Rh(PPh$_3$)$_2$]$^+$ fragment around the carborane cluster.[14] Thus, the electron-rich element not only hampers the formation of *closo* tautomers but also fixes the position of the [Rh(PPh$_3$)$_2$]$^+$ fragment with regard to the carborane cage. Finally, related to this topic is the observation provided by the X-ray structures of [Rh(nH*PPh*)(PPh$_3$)$_2$] and [Rh(nMe*SPh*)(PPh$_3$)$_2$][9] that the [Rh(PPh$_3$)$_2$]$^+$ fragment is bonded to the same B−H group, namely B(11), which is located at the open face. Recent studies[15−17] on the chemistry of (monothiocarborane)- and (monophosphinocarborane)metal complexes have provided evidence that the electron-rich element directly bonded to the cluster's open face enables discrimination between B−H groups. For instance, reaction of the ligand [7-SMe-8-Me-7,8-$C_2B_9H_{10}$]$^-$ with [PdCl$_2$(PPh$_3$)$_2$] led to the formation of [PdCl(7-SMe-8-Me-11-PPh$_2$-7,8-$C_2B_9H_9$)(PPh$_3$)], in which one PPh$_2$ group has been selectively transferred to B(11). Also, in the reaction of monothio- or monophosphinocarborane ligands with [RuCl$_2$(PPh$_3$)$_3$], where the carborane clusters behave as tricoordinating ligands, B(11)−H and B(2)−H are the groups systematically observed to interact with the metal. Nevertheless, we do not have a definitive explanation for the preference of B(11)−H−Rh coordination found in [Rh(nR′*SR*)(PPh$_3$)$_2$] and [Rh(nR′*PR*)(PPh$_3$)$_2$] complexes. Assuming that the formation of S−Rh or P−Rh bonds is favored versus B−H−Rh bonds,[18,19] it is reasonable to expect that the second linkage of the Rh(I) center to the carborane cage will be a B−H group directly connected to the C_{cage}−SR or C_{cage}−PR$_2$ group: that is, B(2), B(3), or B(11). Given the relatively weak donor character of a B−H group, the more electron-rich B(11) vertex belonging to the cluster's open face would appear to be more prone to form a B−H−Rh bond with a coordinatively unsaturated Rh(I) center.

Reaction with Phosphines. [Rh(nMe*SPh*)(PPh$_3$)$_2$] and [Rh(nH*PPh*)(PPh$_3$)$_2$] were chosen as representatives of the two respective *exo-nido*-rhodacarborane families to study their behavior toward the presence of σ-donor ligands in solution.

[Rh(nMe*SPh*)(PPh$_3$)$_2$] reacted readily with PPh$_3$ in CD_2Cl_2 according to ^{1}H{^{11}B}, ^{11}B{^{1}H}, and ^{31}P{^{1}H} NMR spectroscopy. The ^{11}B{^{1}H} and ^{1}H{^{11}B} NMR spectra showed resonances which corresponded to [Rh(nMe*SPh*)(PPh$_3$)$_2$] and free [nMe*SPh*]$^-$, and the respective ^{31}P{^{1}H} NMR spectrum showed signals attributed to the same species. In addition, a new, very broad resonance at ca. 38 ppm appeared which upon cooling to −34 °C was resolved to give two sets of broad resonances centered at 31.3 and 49.8 ppm. Further cooling below −45 °C produced only one extra doublet at 32.4 ppm (^1J(Rh,P) = 133 Hz), which is assigned to the [Rh(PPh$_3$)$_4$]$^+$ species[3] (Figure 8). There exists a strong resemblance between the variable-temperature ^{31}P{^{1}H} NMR spectra of [Rh(nMe*SPh*)(PPh$_3$)$_2$] and those of the non-thioether, *exo-nido* complex [Rh(7-Me-8-Ph-7,8-$C_2B_9H_{10}$)(PPh$_3$)$_2$] reported earlier.[3] At −34 °C the resonances at 31.3 and 49.8 ppm are observed as a doublet (^1J(Rh,P) = 135 Hz) and an unresolved doublet of triplets (^2J(P,P) = ca. 269 Hz), respectively. These

(14) If a migration process was involved, one would expect different sets of resonances in the low-temperature ^{31}P{^{1}H} NMR spectrum belonging to different isomers arising from [Rh(PPh$_3$)$_2$]$^+$ fragments bonded to different B−H sites. However, the spectra show the presence of only one isomer in solution in all the cases studied.

(15) Teixidor, F.; Casabó, J.; Romerosa, A. M.; Viñas, C.; Rius, J.; Miravitlles, C. *J. Am. Chem. Soc.* **1991**, *113*, 9895−9896.
(16) Teixidor, F.; Viñas, C.; Casabó, J.; Romerosa, A. M.; Rius, J.; Miravitlles, C. *Organometallics* **1994**, *13*, 914−919.
(17) Viñas, C.; Nuñez, R.; Teixidor, F.; Kivekäs, R.; Sillanpää, R. *Organometallics* **1996**, *15*, 3850−3858.
(18) Teixidor, F.; Rius, J.; Miravitlles, C.; Viñas, C.; Escriche, Ll.; Sánchez, E.; Casabó, J. *Inorg. Chim. Acta* **1990**, 176, 61−65.
(19) Teixidor, F.; Viñas, C.; Abad, M. M.; Whitaker, C. *Organometallics* **1996**, *14*, 3154−3160.

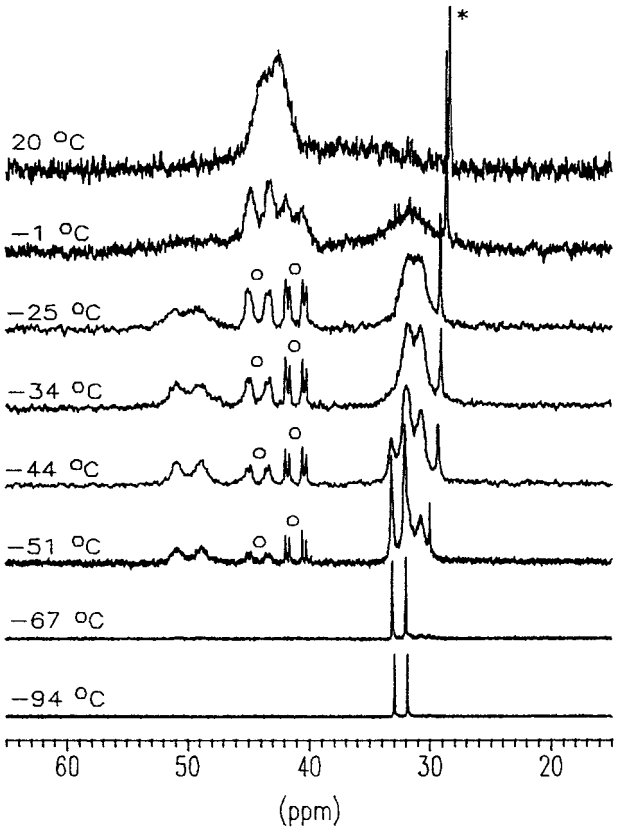

Figure 8. Variable-temperature $^{31}P\{^1H\}$ NMR spectra of the reaction of [Rh(nMe*SPh*)$(PPh_3)_2$] with 3 equiv of PPh_3: (*) $OPPh_3$; (○) [Rh(nMe*SPh*)$(PPh_3)_2$].

two resonances can be tentatively assigned to a T-shaped $[Rh(PPh_3)_3]^+$ species. The large Rh−P coupling constant associated with the resonance at 49.8 ppm could be attributed to the absence of a strong interaction with a trans ligand, and the fourth coordination site would be occupied by either a weakly bonded carborane anion through a single terminal B−H group or a solvent molecule. Besides, the broadness of this signal could be due to hindered rotation of the weakly bonded asymmetric carborane ligand around the $[Rh(PPh_3)_3]^+$ fragment, rendering the phosphorus atoms nonequivalent.

[Rh(nMe*SPh*)$(PPh_3)_2$] was also allowed to react with increasing amounts of the phosphine ligands $PMePh_2$ and PEt_3 in CD_2Cl_2. The two reactions followed the same pattern, which is illustrated in Figures 9 and 10 for the $PMePh_2$ ligand. A doublet in the $^{31}P\{^1H\}$ NMR spectrum (3.7 ppm, ^1J(Rh,P) = 140 Hz) and a broad resonance at −2.3 ppm (B−H−B) in the $^1H\{^{11}B\}$ NMR spectrum belonging to the salt [Rh$(PMePh_2)_4$][nMe*SPh*] were observed even when less than 1 equiv of $PMePh_2$ had been added. As the amount of added $PMePh_2$ was increased, the concentration of the starting complex diminished and that of the salt [Rh$(PMePh_2)_4$][nMe*SPh*] increased. At intermediate ratios between 1:0 and 1:1.5, two new broad doublets at 24.0 ppm and ca. 45.6 ppm in the $^{31}P\{^1H\}$ NMR spectrum were observed. Also, in the $^1H\{^{11}B\}$ NMR spectrum two new broad resonances at ca. −2.7 and −4.3 ppm (which were overlapped with those of the starting complex) appeared. These new signals suggested the formation of a new *exo-nido*-rhodacarborane complex resulting from substitution of PPh_3 ligands in [Rh(nMe*SPh*)$(PPh_3)_2$] by $PMePh_2$ ligands. However, this species was a minor one in every

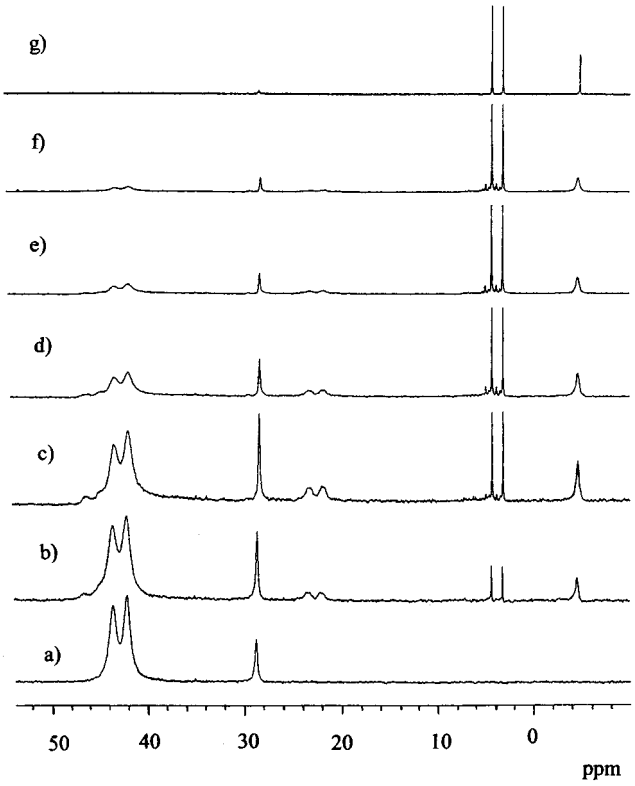

Figure 9. $^{31}P\{^1H\}$ NMR spectra of the reaction of [Rh(nMe*SPh*)$(PPh_3)_2$] with $PMePh_2$ at different [Rh(nMe*SPh*)$(PPh_3)_2$]:$PMePh_2$ ratios: (a) 1:0; (b) 1:0.16; (c) 1:0.33; (d) 1:0.5; (e) 1:0.8; (f) 1:1; (g) 1:1.5.

stage of the reaction and can be regarded as an intermediate species in the reaction that leads to the formation of the [Rh$(PMePh_2)_4$][nMe*SPh*] salt. Analogously, the salt [Rh$(PEt_3)_4$][nMe*SPh*] (d, 9.8 ppm, ^1J(Rh,P) = 136 Hz) was the main product of the reaction of [Rh(nMe*SPh*)$(PPh_3)_2$] with PEt_3.

Unlike [Rh(nMe*SPh*)$(PPh_3)_2$], the reaction of [Rh(nH*PPh*)$(PPh_3)_2$] with PPh_3 in CD_2Cl_2 showed no reaction within 12 h according to ^1H, $^{11}B\{^1H\}$, and $^{31}P\{^1H\}$ NMR spectroscopy. Also, the reaction of [Rh(nH*PPh*)$(PPh_3)_2$] with increasing amounts of PEt_3 in CD_2Cl_2 revealed a different behavior compared to that observed for the thioether complex. The kinetics of the reaction was relatively slow, and 6 h was necessary to achieve equilibrium after each addition of PEt_3. The $^{31}P\{^1H\}$ and $^1H\{^{11}B\}$ NMR spectra are found in Figures 11 and 12. When the ratio [Rh(nH*PPh*)$(PPh_3)_2$]:PEt_3 was 1:0.66, three new sets of resonances appeared at 46.2 (br d, ^1J(Rh,P) = 217 Hz), 14.8 (ddd, $^{trans}J$(P,P) = 284 Hz, ^1J(Rh,P) = 124 Hz, ^{cis}J(P,P) = 35 Hz), and 3.6 ppm (ddd, $^{trans}J$(P,P) = 284 Hz, ^1J(Rh,P) = 119 Hz, ^{cis}J(P,P) = 42 Hz). The resonances at 46.2 and 3.6 ppm are close to those of the starting complex, while that at 14.8 ppm has shifted considerably. Again, the high Rh−P coupling constant of the resonance at 46.2 ppm along with its broadness are indicative of a phosphorus ligand trans to a B−H group. Also, new resonances in the $^1H\{^{11}B\}$ NMR spectrum at −2.83 (B−H−B) and −4.86 ppm (B−H−Rh) were observed. Thus, these new sets of resonances must belong to the mixed phosphine complex [Rh(nH*PPh*)$(PPh_3)(PEt_3)$], which results from the substitution of the PPh_3 ligand trans to the $C_{cage}-PPh_2$ group by a PEt_3 ligand. When the ratio was 1:1, a new

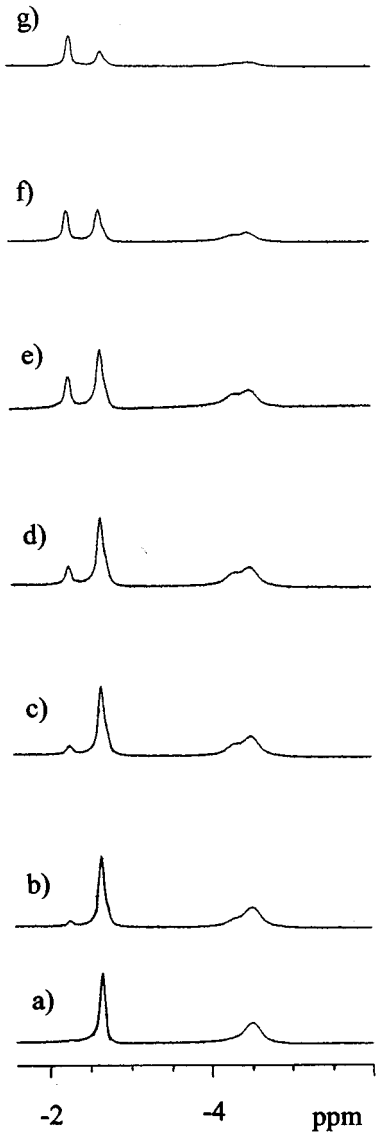

Figure 10. $^1H\{^{11}B\}$ NMR spectra of the reaction of [Rh(nMe*SPh*)(PPh_3)$_2$] with $PMePh_2$ at different [Rh(nMe*SPh*)(PPh_3)$_2$]:$PMePh_2$ ratios: (a) 1:0; (b) 1:0.16; (c) 1:0.33; (d) 1:0.5; (e) 1:0.8; (f) 1:1; (g) 1:1.5.

set of three resonances appeared at 31.4 (br d, ^1J(Rh,P) = 169 Hz), 19.5 (ddd, $^{trans}J$(P,P) = 287 Hz, ^1J(Rh,P) = 129 Hz, ^{cis}J(P,P) = 37 Hz), and 3.8 ppm (ddd, $^{trans}J$(P,P) = 287 Hz, ^1J(Rh,P) = 119 Hz, ^{cis}J(P,P) = 33 Hz). In this case the resonance at 31.4 ppm has shifted significantly from that of the initial complex, suggesting that the PPh_3 ligand trans to the B−H group has been substituted by a PEt_3 ligand. Also, the respective $^1H\{^{11}B\}$ NMR spectra revealed two new resonances at −2.89 ppm (B−H−B, overlapped) and −5.02 ppm (B−H−Rh). The new sets of resonances are attributable to the complex [Rh(nH*PPh*)(PEt_3)$_2$], where the two PPh_3 ligands have been substituted by two PEt_3 ligands. Only when the ratio was 1:2 did the resonances of the salt [Rh(PEt_3)$_4$][nH*PPh*] appear, but even at the ratio 1:3, [Rh(nH*PPh*)(PEt_3)$_2$] was still the main product in the reaction mixture, as was calculated from the integration of the $^1H\{^{11}B\}$ NMR spectrum.

The reaction of [Rh(nH*PPh*)(PPh_3)$_2$] with increasing amounts of phosphine ligands PMe_2Ph and $PMePh_2$ in CD_2Cl_2 proceeded in an analogous manner to that of PEt_3. However, when PMe_2Ph was used a much slower substitution kinetics was observed, since 12 h was needed to achieve equilibrium after each addition. Resonances in the $^{31}P\{^1H\}$ NMR spectrum attributable to the mixed phosphine complex [Rh(nH*PPh*)(PPh_3)(PMe_2Ph)] appeared at 47.5 (^1J(P,Rh) = 199 Hz), 7.3 ($^{trans}J$(P,P) = 298 Hz, ^1J(P,Rh) = 119 Hz, ^{cis}J(P,P) = 39 Hz), and −4.0 ppm ($^{trans}J$(P,P) = 298 Hz, ^1J(P,Rh) = 125 Hz, ^{cis}J(P,P) = 37 Hz) and in the $^1H\{^{11}B\}$ NMR spectrum at −2.7 (B−H−B) and −4.20 ppm (B−H−Rh). For $PMePh_2$, the $^{31}P\{^1H\}$ NMR resonances attributable to [Rh(nH*PPh*)(PPh_3)($PMePh_2$)] appeared at ca. 47.0 (b, ^1J(P,Rh) = 199 Hz), 10.7 ($^{trans}J$(P,P) = 292 Hz, ^1J(P,Rh) = 127 Hz, ^{cis}J(P,P) = 35 Hz), and 6.2 ppm ($^{trans}J$(P,P) = 292 Hz, ^1J(P,Rh) = 125 Hz, ^{cis}J(P,P) = 37 Hz) and the $^1H\{^{11}B\}$ NMR resonances at −3.0 (B−H−B) and −4.5 ppm (B−H−Rh).

These reactions are indicated in Figure 13. In summary, the reactions of [Rh(nMe*SPh*)(PPh_3)$_2$] with different phosphine ligands lead to displacement of the carborane ligand from the coordination sphere of the metal. This behavior parallels that observed for *exo-nido*-rhodacarborane complexes with no electron-rich substituents on the cluster. In contrast, when [Rh(nH*PPh*)(PPh_3)$_2$] is allowed to react with the same phosphine ligands, only the ancillary PPh_3 ligands are substituted at complex:phosphine ratios between 1:1 and 1:3. Also, the order of substitution is in agreement with the trans influence observed in the X-ray study.

Catalytic Hydrogenation. The rhodacarboranes with no electron-rich substituents have shown to be active catalysts in a variety of processes.[6−8,20−22] Due to the notable resemblance between the *exo-nido*-rhodacarboranes presented in this paper and those developed earlier, we started a study of their possible catalytic applications to learn of the benefits of incorporating the coordinating electron-rich element on the cluster carbon atom. At this level we have been interested in semiquantitative or gross features of the catalytic systems for the purpose of comparison. Thus, although no detailed mechanistic investigation has been yet performed that allows a full discussion, the following trends have emerged from the experiments performed to date. In Table 4 we have gathered the percentage of hydrogenation and isomerization of 1-hexene at different pressures and temperatures after 1 h of reaction for the complexes belonging to the [Rh(nR′*SR*)(PPh_3)$_2$] and [Rh(nR′*PR*)(PPh_3)$_2$] families.

The two families of rhodacarborane complexes [Rh(nR′*SR*)(PPh_3)$_2$] and [Rh(nR′*PR*)(PPh_3)$_2$] exhibit marked differences with regard to their catalytic activities in the hydrogenation of 1-hexene. While the (monothiocarborane)rhodium complexes are active catalysts under mild conditions (P = 1 bar, T = 25 °C), the monophosphino compounds require higher pressures and temperatures. Differences in activity have also been observed between different complexes belonging to the same family. Entries 1−3 contain conversions to hexane and

(20) Zakharkin, L. I.; Chizhevsky, I. T.; Zhigareva, G. G.; Petrovskii, P. V.; Polyakov, A. V.; Yanovsky, A. I.; Struchkov, Y. T. *J. Organomet. Chem.* **1988**, *358*, 449.
(21) Kang, H. C.; Hawthorne, M. F. *Organometallics* **1990**, *9*, 2327−2332.
(22) Pirotte, B.; Felekidis, A.; Fontaine, M.; Demonceau, A.; Noels, A. F.; Delarge, J.; Chizhevsky, I. T.; Zinevich, T. V.; Pisareva, I. V.; Bregadze, V. I. *Tetrahedron Lett.* **1993**, *34*, 1471−1474.

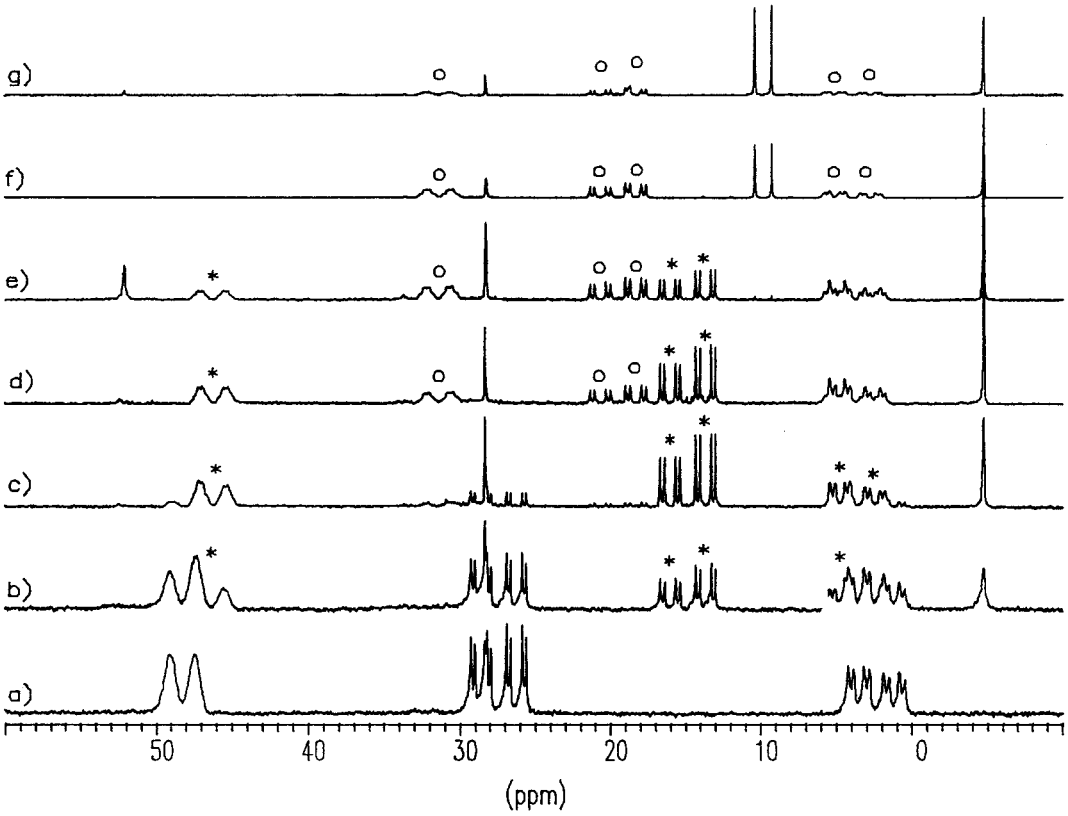

Figure 11. $^{31}P\{^1H\}$ NMR spectra of the reaction of [Rh(nH*PPh*)(PPh_3)$_2$] with PEt_3 at different [Rh(nH*PPh*)(PPh_3)$_2$]:PEt_3 ratios: (a) 1:0; (b) 1:0.33; (c) 1:0.66; (d) 1:1; (e) 1:1.5; (f) 1:2; (g) 1:3; (*) [Rh(nH*PPh*)(PPh_3)(PEt_3)]; (○) [Rh(nH*PPh*)(PEt_3)$_2$].

2-hexenes obtained using [Rh(nR′*SR*)(PPh_3)$_2$] at $P = 1$ bar and 25 °C. Similar experiments were performed with the well-known rhodium catalyst [RhCl(PPh_3)$_3$] (Wilkinson's catalyst) for comparison (entry 4). Remarkably, [Rh(nMe*SPh*)(PPh_3)$_2$] exhibits a much higher conversion to hexane than the rest, being ca. 8 times higher than Wilkinson's catalyst. Although not so active, complex [Rh(nMe*SEt*)(PPh_3)$_2$] presents ca. 2.5 times higher conversion to hexane than [RhCl(PPh_3)$_3$]. Interestingly, isomerization to 2-hexenes turns out to be the main reaction occurring with [Rh(nPh*SPh*)(PPh_3)$_2$]. In our preliminary communication we claimed that the high activity presented by [Rh(nMe*SPh*)(PPh_3)$_2$] could be due to the unique stereochemistry of the complex. This hypothesis was based on an earlier mechanistic investigation of rhodacarborane-catalyzed hydrogenations,[8] where evidence was provided that the B−H groups belonging to the open face (upper belt) were more prone to undergo B−Rh^{III}−H oxidative addition during the catalytic cycle and thus provoke enhanced rates. The high activity observed for the [Rh(nR′*SR*)(PPh_3)$_2$] family would seem to support this hypothesis. Nevertheless, although this possibility cannot be ruled out, the marked differences in rates observed between the thioether and phosphino complexes indicate that other important factors must be operating.

The temperature of the reaction affects the two families differently. In both families, higher temperatures result in increasing ratios of isomerization to hydrogenation (compare entries 5 and 10, and entries 6−9 and 11−14). However, while the use of ambient temperatures results in a higher *n*-hexane yield for [Rh(nMe*SPh*)(PPh_3)$_2$], the activity of complexes of the [Rh-

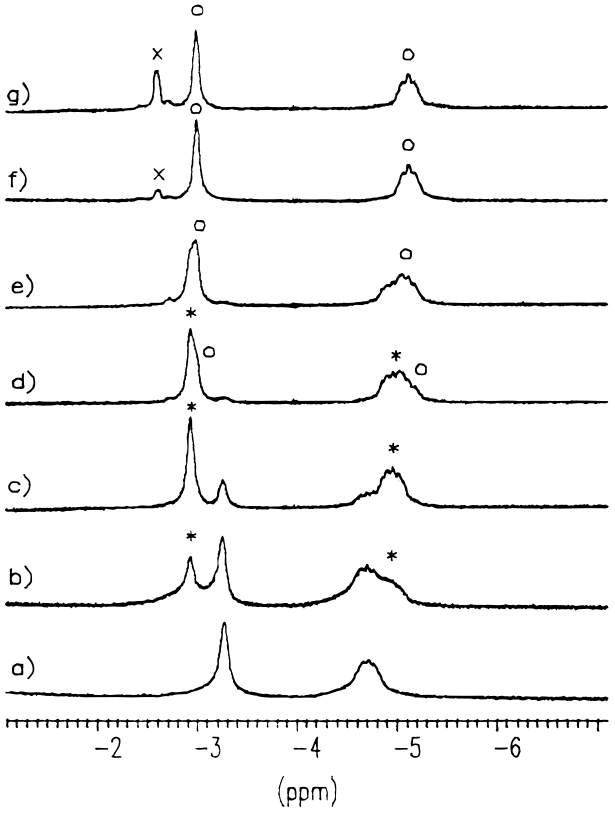

Figure 12. $^1H\{^{11}B\}$ NMR spectra of the reaction of [Rh(nH*PPh*)(PPh_3)$_2$] with PEt_3 at different [Rh(nH*PPh*)(PPh_3)$_2$]:PEt_3 ratios: (a) 1:0; (b) 1:0.33; (c) 1:0.66; (d) 1:1; (e) 1:1.5; (f) 1:2; (g) 1:3; (*) [Rh(nH*PPh*)(PPh_3)(PEt_3)]; (○) [Rh(nH*PPh*)(PEt_3)$_2$]; (×) [Rh(PEt_3)$_4$][nH*PPh*].

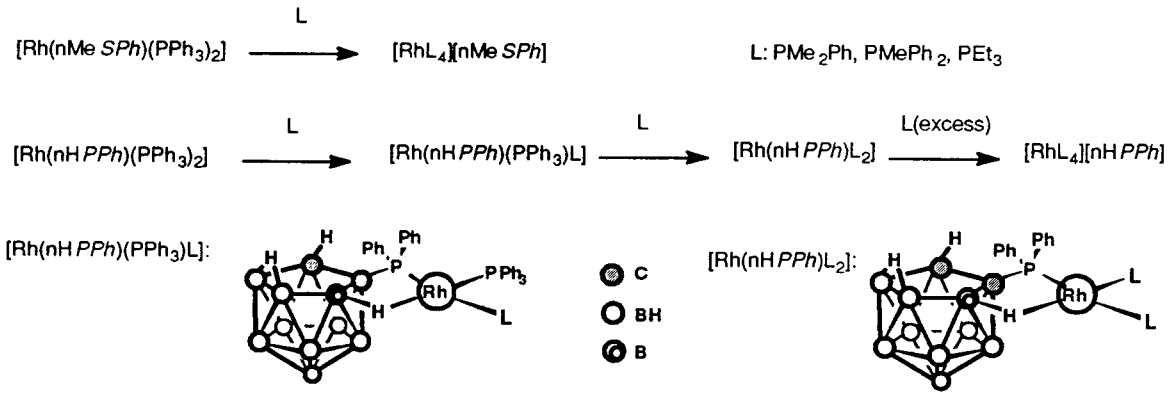

Figure 13. Reactions of [Rh(nMe*SPh*)(PPh_3)$_2$] and [Rh(nH*PPh*)(PPh_3)$_2$] with phosphines.

Table 4. Percent Conversion of 1-Hexene to Hexane and 2-Hexenes after 1 h of Reaction[a]

entry no.	complex	*T* (°C)	*P* (bar)	10^4[Cat] (M)	[1-hexene] (M)	% hexane	% 2-hexenes
1	(Rh(nMe*SPh*)(PPh_3)$_2$]	25	1	7.4	1.1	47	9
2	(Rh(nMe*SEt*)(PPh_3)$_2$]	25	1	7.4	1.1	14	5.3
3	(Rh(nPh*SPh*)(PPh_3)$_2$]	25	1	7.4	1.1	3.6	12
4	($RhCl(PPh_3)_3$]	25	1	7.4	1.1	6	0.4
5	(Rh(nMe*SPh*)(PPh_3)$_2$]	25	45	5.2	3.9	98	2.0
6	(Rh(nH*PPh*)(PPh_3)$_2$]	25	45	5.2	3.9	12	0.7
7	(Rh(nMe*PPh*)(PPh_3)$_2$]	25	45	5.2	3.9	6	0.3
8	(Rh(nMe*PEt*)(PPh_3)$_2$]	25	45	5.2	3.9	0.2	0.1
9	(Rh(nMeP^i*Pr*)(PPh_3)$_2$]	25	45	5.2	3.9	2.4	0.1
10	(Rh(nMe*SPh*)(PPh_3)$_2$]	66	45	5.2	3.9	85	11
11	(Rh(nH*PPh*)(PPh_3)$_2$]	66	45	5.2	3.9	90	9.3
12	(Rh(nMe*PPh*)(PPh_3)$_2$]	66	45	5.2	3.9	61	20
13	(Rh(Me*PEt*)(PPh_3)$_2$]	66	45	5.2	3.9	82	11
14	(Rh(nMeP^i*Pr*)(PPh_3)$_2$]	66	45	5.2	3.9	83	14

[a] Yields represent averaged values for at least two runs. The experiments in entries 1−4 were performed using toluene as solvent. THF was used in the rest (entries 5−14).

(nR′*PR*)(PPh_3)$_2$] family fall dramatically if ambient temperatures are used.

On the other hand, both catalytic systems were shown to be recoverable upon completion of the catalytic reactions, as shown by $^1H\{^{11}B\}$, $^{11}B\{^1H\}$, and $^{31}P\{^1H\}$ NMR spectroscopy. Both families exhibited no sign of deactivation and eventually converted all the 1-hexene into hexane and 2-hexenes. The hydrogenation of 2-hexenes proceeded much more slowly than for 1-hexene, but they were eventually hydrogenated, provided that high H_2 pressures were applied. Finally, the catalytic activity of both families was inhibited when PPh_3 was added to the reaction mixture.

At this point we want to emphasize that the different behavior observed in the reaction of complexes [Rh(nMe*SPh*)(PPh_3)$_2$] and [Rh(nH*PPh*)(PPh_3)$_2$] with phosphine ligands may have important consequences in the future application of these complexes as catalysts. It is desirable for a catalyst system to be robust toward the presence of donor atoms belonging to the substrate, especially where a degree of selectivity is required.[23] From this point of view, complexes belonging to the [Rh(nR′*PR*)(PPh_3)$_2$] family seem to fulfill this requirement better than the sulfur analogues. Following these considerations, we have started to explore the utility of the catalyst systems reported in this paper in stereoselective catalytic transformations. In this regard, the introduction of chirality in drugs in the course of their synthesis is a subject of particular importance. A recent report[22] on the hydrogenation of methacycline to doxycycline using the rhodacarborane complex [closo-3,3-(η^2:η^3-$C_7H_7CH_2$)-3,1,2-$RhC_2B_9H_{11}$] attracted our attention on account of the high diastereoselectivity (close to 95%) reported, being equal or superior to that reported for patent systems.[24] Doxycycline is a potent tetracycline antibiotic extensively used in chemotherapy.[25] The hydrogenation of methacycline can lead to the formation of two diastereomers: doxycycline and *epi*-doxycycline (Figure 14). We wondered if the complexes developed in this paper could perform in a similar way. For that purpose, [Rh(nMe*PPh*)(PPh_3)$_2$] and [Rh(nH*PPh*)(PPh_3)$_2$] were tested as catalyst precursors and they were shown to hydrogenate the antibiotic precursor methacycline, exhibiting high conversions (85 and 99.7% yields, respectively) with very high diastereoselectivity for the

(23) For instance, in the asymmetric hydrogenation of α-(acylamino)-acrylic acids by [Rh(binap)(COD)]ClO_4, the use of a high substrate to catalyst ratio results in a low enantiomeric excess due to substitution reactions: Miyashita, A.; Takaya, H.; Souchi, T.; Noyori, R. *Tetrahedron* **1984**, *40*, 1245−1253.

(24) (a) Broggi, R.; Cotti, G. (Ankerfarm SpA) German Patent 2308227, August 30, 1973; *Chem. Abstr.* **1973**, *79*, 136908r. (b) Brennan, T. M.; Faubl, H. (Pfizer Inc.) German Patent 2403714, August 22, 1974; *Chem. Abstr.* **1975**, *82*, 43099z. (c) Cotti, G. (Ankerfarm SpA) German Patent 2446587, April 3, 1975; *Chem. Abstr.* **1975**, *83*, 114090y. (d) Page, P. R.; Villax, I.; (Plurichemie Anstalt) US Patent 4743699, May 10, 1988; *Chem. Abstr.* **1989**, *110*, 2142494d. (e) Heggie, W.; Hursthouse, M. B.; Page, P. R.; Somerville, R. G.; Villax, I. (Plurichemie Anstalt) European Pat. Appl. EP 283615, September 28, 1988; *Chem. Abstr.* **1989**, *110*, 78059k. (f) Heggie, W.; Page, P. R.; Villax, I.; Ghatak, I.; Hursthouse, M. B. (Plurichemie Anstalt) European Pat. Appl. EP 283616, September 28, 1988; *Chem. Abstr.* **1989**, *110*, 64523v.

(25) (a) Wolf, M. E., Ed. *Burger's Medicinal Chemistry*, 4th ed.; Wiley: New York, 1979; Vol. 2 (Nonlactam Antibiotics), p 226. (b) Korolkovas, A. *Essentials of Medicinal Chemistry: Chemothempeutics Agents-Anti-infective Agents*, 2nd ed.; Wiley-Interscience: New York, 1988; p 797.

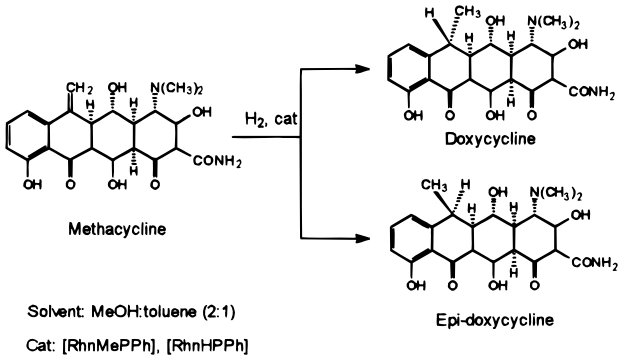

Figure 14. Hydrogenation of methacycline to doxycycline and *epi*-doxycycline.

pharmacologically important doxycycline molecule (ca. 100%). The other possible diastereoisomer *epi*-doxycycline was not observed in any case. These results open a promising area of research on stereoselective transformations catalyzed by the rhodacarboranes reported here and are currently under investigation in our research group.

Experimental Section

Instrumentation. Elemental analyses were performed using a Carlo Erba EA1108 microanalyzer. IR spectra were recorded with KBr pellets on a Nicolet 710 FT spectrophotometer. The ^{1}H NMR, ^{31}P NMR, and ^{11}B NMR spectra were recorded using a Bruker ARX 300 instrument. Catalytic hydrogenations were conducted in a 35-mL autoclave built at the workshop facility of the Universitat Autònoma de Barcelona. The autoclave was equipped with a water jacket, a rupture disk, a manometer, and sample and gas inlets. GC analyses were performed with a Shimadzu GC-15A instrument using an SPB-1 capillary column (Supelco; 30 m in length, 0.25 mm inner diameter, and 1 μm thickness stationary phase). HPLC analyses were conducted using a Perkin-Elmer chromatograph equipped with a 410 LC pump and a LC-235 diode-array detector.

Materials. Unless otherwise noted, all manipulations were carried out under a dinitrogen atmosphere using standard vacuum line techniques. THF and toluene were distilled from sodium benzophenone prior to use. 1-Hexene (Aldrich) was freshly distilled from CaH_2 prior to use. The rest of the solvents were of reagent grade quality and were used without further purification. Decaborane, *o*-carborane, and methyl-*o*-carborane (Dexsil Chemical Corp.), $RhCl_3 \cdot 3H_2O$ (Johnson Matthey), and $PMePh_2$, PMe_2Ph, and PEt_3 (Aldrich) were purchased from commercial sources and used as received. PPh_3 (Aldrich) was recrystallized from ethanol before use. Deuterated solvents for NMR (Fluorochem) were freeze−pump−thawed three times under N_2 and transferred to the NMR tube using standard vacuum line techniques. Tetraalkylammonium salts of [nR′*PR*]$^-$,[26] cesium salts of [nR′*SR*]$^-$,[16] and [RhCl(PPh$_3$)$_3$][27] were prepared according to the literature methods.

Synthesis of [Rh(nMe*SPh*)(PPh$_3$)$_2$]. A solution of Cs[nMe*SPh*] (90 mg, 0.23 mmol) and [RhCl(PPh$_3$)$_3$] (202 mg, 0.22 mmol) in toluene−ethanol (8:1, 28 mL) was stirred at room temperature for 6 h (in our preliminary communication[9] we reported a reaction time of 18 h, but we have observed that 6 h is enough to achieve completion of reaction). The white precipitate of CsCl formed was filtered through Celite, the orange solution was concentrated under vacuum to 4 mL, and ethanol (20 mL) was added, affording a red solid which was washed with ethanol (2 × 5 mL) and ether (2 × 5 mL) and dried under vacuum. Yield: 176 mg (90%). Sometimes the complex precipitated as an orange solid which, upon stirring, slowly converted to the red crystalline form. The elemental composition and spectroscopic properties of both orange and red forms were identical. IR (KBr; ν, cm^{-1}): 2527 (B−H), 2112 (B−H−Rh). ^{1}H NMR (300 MHz, CD_2Cl_2, 25 °C, TMS; δ): 7.66−7.11 (m, 35H, aryl), 1.48 (s, 3H, CH_3), −2.69 (br, 1H, B−H−B), −4.55 (br, 1H, B−H−Rh). ^{11}B NMR (96.3 MHz, CD_2Cl_2, 25 °C, $Et_2O \cdot BF_3$; δ): −7.9 (1B), −10.9 (2B), −13.8 (1B), −18.5 (d, ^1J(B−H) = 86 Hz, 1B), −23.0 (1B), −24.5 (1B), −29.1 (1B), −35.9 (d, ^1J(B−H) = 137 Hz, 1B). ^{31}P{^{1}H} NMR (121.5 MHz, CD_2Cl_2, 25 °C, H_3PO_4, 85%; δ): 42.8 (br d, ^1J(Rh,P) =176 Hz). ^{31}P{^{1}H} NMR (121.5 MHz, CD_2Cl_2, −94 °C, H_3PO_4, 85%; δ): 44.0 (dd, ^1J(Rh,P) = 187 Hz, ^2J(P,P) = 40 Hz), 41.2 (dd, ^1J(Rh,P) = 165 Hz, ^2J(P,P) = 40 Hz). Anal. Calcd for $C_{45}H_{48}B_9P_2SRh$: C, 61.20; H, 5.48; S, 3.60. Found: C, 61.15; H, 5.44; S, 3.07.

Synthesis of [Rh(nPh*SPh*)(PPh$_3$)$_2$]. A method similar to the one described for the preparation of [Rh(nMe*SPh*)(PPh$_3$)$_2$] was employed: Cs[nPh*SPh*] (100 mg, 0.22 mmol), [RhCl(PPh$_3$)$_3$] (195 mg, 0.21 mmol), toluene−ethanol (8:1, 28 mL), 6 h. Yield: 161 mg (83%). IR (KBr; ν, cm^{-1}): 2544 (B−H), 2104 (B−H−Rh). ^{1}H NMR (300 MHz, CD_2Cl_2, 25 °C, TMS; δ): 7.46−6.84 (m, 40H, aryl), −2.38 (br, 1H, B−H−B), −4.40 (br, 1H, B−H−Rh). ^{11}B NMR (96.3 MHz, CD_2Cl_2, 25 °C, $Et_2O \cdot BF_3$; δ): −6.8 (1B), −13.4 (3B), −18.6 (d, ^1J(B−H) = 88 Hz, 1B), −23.3 (1B), −25.3 (1B), −29.4 (1B), −35.9 (d, ^1J(B−H) = 134 Hz, 1B). ^{31}P{^{1}H} NMR (121.5 MHz, CD_2Cl_2, 25 °C, H_3PO_4, 85%; δ): 42.7 (br). ^{31}P{^{1}H} NMR (121.5 MHz, CD_2Cl_2, −94 °C, H_3PO_4, 85%; δ): 48.1 (dd, ^1J(Rh,P) = 193 Hz, ^2J(P,P) = 39 Hz), 37.3 (dd, ^1J(Rh,P) = 158 Hz, ^2J(P,P) = 39 Hz). Anal. Calcd for $C_{50}H_{50}B_9P_2SRh$: C, 63.54; H, 5.33; S, 3.39. Found: C, 60.83; H, 5.11; S, 2.88.

Synthesis of [Rh(nMe*SEt*)(PPh$_3$)$_2$]. A method similar to the one described for the preparation of [Rh(nMe*SPh*)(PPh$_3$)$_2$] was employed: Cs[nMe*SEt*] (100 mg, 0.29 mmol), [RhCl(PPh$_3$)$_3$] (246 mg, 0.27 mmol), toluene−ethanol (8:1, 28 mL), 6 h. Yield: 180 mg (82%). IR (KBr; ν, cm^{-1}): 2555, 2519 (B−H); 1956 (B−H−Rh). ^{1}H NMR (300 MHz, CD_2Cl_2, 25 °C, TMS; δ): 7.51−7.18 (m, 30H, aryl), 1.60 (q, 2H, S−CH_2−CH_3), 1.45 (s, 3H, C_{cage}−CH_3), 0.72 (t, 3H, S−CH_2−CH_3), −2.51 (br, 1H, B−H−Rh), −4.73 (br, 1H, B−H−Rh). ^{11}B{^{1}H} NMR (96.3 MHz, CD_2Cl_2, 25 °C, $Et_2O \cdot BF_3$; δ): −8.6 (1B), −11.6 (2B), −15.0 (1B), −19.9 (d, ^1J(B−H) = 91 Hz, 1B), −25.6 (d, ^1J(B−H) = 127 Hz, 2B), −29.3 (1B), −36.8 (d, ^1J(B−H) = 136 Hz, 1B).^{31}P{^{1}H} NMR (121.5 MHz, CD_2Cl_2, 25 °C, H_3PO_4, 85%; δ): 42.6 (br d, ^1J(Rh,P) =180 Hz). ^{31}P{^{1}H} NMR (121.5 MHz, CD_2Cl_2, −94 °C, H_3PO_4, 85%; δ): 43.0 (dd, ^1J(Rh,P) = 187 Hz, ^2J(P,P) = 40 Hz), 42.1 (dd, ^1J(Rh,P) = 165 Hz, ^2J(P,P) = 40 Hz). Anal. Calcd for $C_{41}H_{48}B_9P_2SRh$: C, 58.97; H, 5.79; S, 3.84. Found: C, 59.54; H, 5.69; S, 3.30.

Synthesis of [Rh(nH*PPh*)(PPh$_3$)$_2$]. To 20 mL of deoxygenated ethanol containing 75 mg (0.19 mmol) of [NMe$_4$][nH*PPh*] was added [RhCl(PPh$_3$)$_3$] (177 mg, 0.19 mmol), and the mixture was heated to reflux. After ca. 0.5 h, an orange solid precipitated in the warm mixture. The suspension was cooled to room temperature, and the resulting orange solid was isolated by filtration, washed with cool ethanol (6 mL) and ether (15 mL), and dried under vacuum. Yield: 138 mg (77%). IR (KBr; ν, cm^{-1}): 2593, 2537 (B−H), 2129 (B−H−Rh). ^{1}H NMR (300 MHz, CD_2Cl_2, 25 °C, TMS; δ): 7.75−6.65 (m, 40H, aryl), −3.20 (br, 1H, B−H−B), −4.70 (br d, ^1J(B−H) = 86 Hz, 1H, B−H−Rh). ^{11}B NMR (96.3 MHz, CD_2Cl_2, 25 °C, $Et_2O.BF_3$; δ): −3.5 (1B), −14.1 (3B), −16.7 (d, ^1J(B−H) = 86 Hz, 1B), −24.4 (2B), −29.1 (d, ^1J(B−H) = 106 Hz, 1B), −35.1 (d, ^1J(B−H) = 144 Hz, 1B). ^{31}P{^{1}H} NMR (121.5 MHz, CD_2Cl_2, 25 °C, H_3PO_4, 85%; δ): 48.06 (br d, ^1J(Rh,P) = 199 Hz, PPh_3). 27.43 (ddd, ^2J(P,P) = 282 Hz, ^1J(Rh,P) = 159 Hz, ^2J(P,P) = 31 Hz, PPh_3), 2.31 (ddd, ^2J(P,P) = 282 Hz, ^1J(Rh,P) = 169 Hz, ^2J(P,P)

(26) Teixidor, F. T.; Viñas, C.; Abad, M. M.; Nuñez, R.; Kivekäs, R.; Sillanpää, R. *J. Organomet. Chem.* **1995**, *503*, 193.
(27) Osborn, J. A.; Wilkinson, G. *Inorg. Synth. 10*, 67.

= 43 Hz, BC−PPh_2). Anal. Calcd for $C_{50}H_{53}B_9P_3Rh$: C, 63.55; H, 5.44. Found: C, 62.19; H, 5.26.

Synthesis of [Rh(nMe*PPh*)(PPh_3)$_2$]. The procedure was as for [Rh(nH*PPh*)(PPh_3)$_2$], but the solid was filtered while hot: [NMe_4][nMe*PPh*] (100 mg, 0.25 mmol), [RhCl(PPh_3)$_3$] (227 mg, 0.25 mmol), ethanol (60 mL), 4 h. Yield: 200 mg (84%). IR (KBr; ν, cm^{-1}): 2579, 2544, 2492 (B−H), 2101 (B−H−Rh). ^{1}H NMR (300 MHz, $CDCl_3$, 25 °C, TMS; δ): 7.75−6.85 (m, 40H, aryl), 0.98 (s, 3H, CH_3), −3.12 (br, 1H, B−H−B), −4.70 (br d, ^1J(B−H) = 86 Hz, 1H, B−H−Rh), ^{11}B NMR (96.3 MHz, $CDCl_3$, 25 °C, $Et_2O{\cdot}BF_3$; δ): −5.5 (1B), −8.3 (d, ^1J(B−H) = 131 Hz, 1B), −12.9 (2B), −15.7 (d, ^1J(B−H) = 86 Hz, 1B), −24.3 (d, ^1J(B−H) = 112 Hz, 2B), −30.2 (1B), −35.6 (d, ^1J(B−H) = 128 Hz, 1B). ^{31}P{^{1}H} NMR (121.5 MHz, $CDCl_3$, 25 °C, H_3PO_4, 85%; δ): 50.1 (br d, ^1J(P,Rh) = 208 Hz, PPh_3), 30.20 (ddd, ^2J(P,P) = 283 Hz, ^1J(Rh,P) = 128 Hz, ^2J(P,P) = 32 Hz, PPh_3), 4.55 (ddd, ^2J(P,P) = 283 Hz, ^2J(Rh,P) = 124 Hz, ^2J(P,P) = 41 Hz, BC−PPh_2). Anal. Calcd for $C_{51}H_{53}B_9P_3Rh$: C, 63.89; H, 5.53. Found: C, 63.15; H, 5.37.

Synthesis of [Rh(nPh*PPh*)(PPh_3)$_2$]. The procedure was as for [Rh(nMe*PPh*)(PPh_3)$_2$]: [NBu_4][nPh*PPh*] (65.0 mg, 0.10 mmol), [RhCl(PPh_3)$_3$] (94.5 mg, 0.10 mmol), ethanol (15 mL), 3 h. After isolation, the solid was washed with ethanol (10 mL) and recrystallized in acetone−ethanol. Yield: 45 mg (43%). IR (KBr; ν, cm^{-1}): 2551, 2509 (B−H), 2101 (B−H−Rh). ^{1}H NMR (300 MHz, $CDCl_3$, 25 °C, TMS; δ): 7.74−6.65 (m, 45H, aryl), −2.55 (br, 1H, B−H−B), −3.68 (br d, ^1J(B−H) = 96 Hz, 1H, B−H−Rh). ^{11}B NMR (96.3 MHz, $CDCl_3$, 25 °C, $Et_2O{\cdot}BF_3$; δ): −2.1 (1B), −8.5 (2B), −13.2 (d, ^1J(B−H) = 96 Hz, 2B), −22.9 (d, ^1J(B−H) = 106.7 Hz, 2B), −27.7 (1B), −33.3 (d, ^1J(B−H) = 124.4 Hz, 1B). ^{31}P{^{1}H} NMR (121.5 MHz, $CDCl_3$, 25 °C, H_3PO_4, 85%; δ): 46.51 (br d, ^1J(P,Rh) = 197 Hz, PPh_3), 28.28 (ddd, ^2J(P,P) = 281 Hz, ^1J(Rh,P) = 128 Hz, ^2J(P,P) = 33 Hz, PPh_3), 6.64 (ddd, ^2J(P,P) = 281 Hz, ^1J(Rh,P) = 123 Hz, ^2J(P,P) = 40 Hz, BC−PPh_2). Anal. Calcd for $C_{56}H_{55}B_9P_3Rh$: C, 65.87; H, 5.43. Found: C, 64.90; H, 5.15.

Synthesis of [Rh(nMe*PEt*)(PPh_3)$_2$]. The procedure was as for [Rh(nMe*PPh*)(PPh_3)$_2$]: [NBu_4][nMe*PEt*] (75.0 mg, 0.16 mmol), [RhCl(*PPh*$_3$)$_3$] (145 mg, 0.16 mmol), ethanol (20 mL), 3 h. After isolation, the solid was washed with ethanol (15 mL) and dried under vacuum. Yield: 75 mg (55%). IR (KBr; ν, cm^{-1}): 2551, 2523 (B−H), 1960 (B−H−Rh). ^{1}H NMR (300 MHz, $CDCl_3$, 25 °C, TMS; δ): 7.74−7.14 (m, 30H, aryl), 1.76 (m, 4H, C*H*$_2$−CH_3), 1.27 (s, 3H, BC−CH_3), 1.24 (m, 3H, CH_2−C*H*$_3$), 0.90 (m, 3H, CH_2−C*H*$_3$), −3.04 (br, 1H, B−H−B), −4.87 (br d, ^1J(B−H) = 96 Hz, 1H, B−H−Rh). ^{11}B NMR (96.3 MHz, $CDCl_3$, 25 °C, $Et_2O{\cdot}BF_3$; δ): −3.8 (2B), −12.1 (2B), −14.7 (d, ^1J(B−H) = 96 Hz, 1B), −23.0 (d, ^1J(B−H) = 105 Hz, 2B), −28.8 (1B), −34.2 (d, ^1J(B−H) = 125 Hz, 1B). ^{31}P{^{1}H} NMR (121.5 MHz, $CDCl_3$, 25 °C, H_3PO_4, 85%; δ): 50.89 (d, ^1J(P,Rh) = 195 Hz, PPh_3), 27.96 (ddd, ^2J(P,P) = 275 Hz, ^1J(Rh,P) = 124 Hz, ^2J(P,P) = 33 Hz, PPh_3), 8.25 (ddd, ^2J(P,P) = 275 Hz, ^1J(Rh,P) = 123 Hz, ^2J(P,P) = 43 Hz, BC−PEt_2). Anal. Calcd for $C_{43}H_{53}B_9P_3Rh$: C, 59.85; H, 6.19. Found: C, 58.52; H, 5.71.

Synthesis of [Rh(nPh*PEt*)(PPh_3)$_2$]. The procedure was as for [Rh(nMe*PPh*)(PPh_3)$_2$]: [NBu_4][nPh*PEt*] (35 mg, 0.065 mmol), [RhCl(PPh_3)$_3$] (60 mg, 0.065 mmol), ethanol (10 mL), 1 h. After isolation the solid was washed with ethanol (5 mL) and dried under vacuum. Yield: 32 mg (53%). IR (KBr; ν, cm^{-1}): 2586, 2544 (B−H), 2094 (B−H−Rh). ^{1}H NMR (300 MHz, CD_2Cl_2, 25 °C, TMS; δ): 7.65−7.13 (m, 35H, aryl), 1.63 (m, 4H, C*H*$_2$−CH_3), 0.77 (m, 6H, CH_2−C*H*$_3$), −2.55 (br, 1H, B−H−B), −4.57 (br, 1H, B−H−Rh). ^{11}B NMR (96.3 MHz, CD_2Cl_2, 25 °C, $Et_2O{\cdot}BF_3$; δ): −2.1 (1B), −6.4 (1B), −13.4 (d, ^1J(B−H) = 86 Hz, 3B), −23.2 (d, ^1J(B−H) = 115 Hz, 2B), −28.2 (1B), −33.5 (d, ^1J(B−H) = 134 Hz, 1B). ^{31}P{^{1}H} NMR (121.5 MHz, CD_2Cl_2, 25 °C, H_3PO_4, 85%; δ): 49.96 (d, ^1J(Rh,P) = 195 Hz, PPh_3), 28.50 (ddd, ^2J(P,P) = 275 Hz, ^1J(Rh,P) = 125 Hz, ^2J(P,P) = 34 Hz, PPh_3), 13.57 (ddd, ^2J(P,P) = 275 Hz, ^1J(Rh,P) = 119 Hz, ^2J(P,P) = 43 Hz, BC−PEt_2). Anal. Calcd for $C_{48}H_{55}B_9P_3Rh$: C, 62.32; H, 5.99. Found: C, 61.23; H, 5.60.

Synthesis of [Rh(nMe^i*Pr*)(PPh_3)$_2$]. To 25 mL of deoxygenated ethanol containing 75.0 mg (0.15 mmol) of [NBu_4][nMeP^i*Pr*] was added [RhCl(PPh_3)$_3$] (137 mg, 0.15 mmol), and the mixture was refluxed for 10 h and stirred at room temperature for 2 days, giving a yellow solution. The solution was concentrated, and a yellow solid precipitated which was isolated by filtration under N_2, washed with deoxygenated ethanol (2 × 10 mL), and dried under vacuum. Yield: 30 mg (23%). IR (KBr; ν, cm^{-1}): 2544, 2523 (B−H), 1960 (B−H−Rh). ^{1}H NMR (300 MHz, $CDCl_3$, 25 °C, TMS; δ): 7.95−7.10 (m, 30H, aryl), 2.35 (m, 2H, C*H*−CH_3), 1.76 (m, 3H, CH−C*H*$_3$), 1.70 (s, 3H, BC−CH_3), 1.19 (m, 3H, CH−C*H*$_3$), 0.78 (m, 6H, CH−C*H*$_3$), −3.22 (br, 1H, B−H−B), −5.50 (br d, ^1J(B−H) = 89 Hz, 1H, B−H−Rh). ^{11}B NMR (96.3 MHz, $CDCl_3$, 25 °C, $Et_2O{\cdot}BF_3$; δ): −4.4 (1B), −5.8 (1B), −12.3 (2B), −13.9 (d, ^1J(B−H) = 89 Hz, 1B), −22.5 (d, ^1J(B,H) = 115 Hz, 2B), 29.1 (1B), −33.9 (d, ^1J(B−H) = 128 Hz, 1B). ^{31}P{^{1}H} NMR (121.5 MHz, $CDCl_3$, 25 °C, H_3PO_4, 85%; δ): 49.17 (d, ^1J(Rh,P) = 207 Hz, PPh_3), 28.29 (ddd, ^2J(P,P) = 275 Hz, ^1J(Rh,P) = 119 Hz, ^2J(P,P) = 40 Hz, PPh_3), 24.29 (ddd, ^2J(P,P) = 275 Hz, ^1J(Rh,P) = 123 Hz, ^2J(P,P) = 35 Hz, BC−P^{i}Pr$_2$). Anal. Calcd for $C_{45}H_{57}B_9P_3Rh$: C, 60.69; H, 6.40. Found: C, 60.95; H, 6.40.

Reactions of [Rh(nMe*SPh*)(PPh_3)$_2$] and [Rh(nH*PPh*)(PPh_3)$_2$] with Phosphines. These reactions were monitored by ^{1}H{^{11}B}, ^{31}P{^{1}H}, and ^{11}B{^{1}H} NMR spectroscopy. The complex was weighed in a Schlenk flask and the deuterated solvent was added forming a clear solution. The solution was transferred to a NMR tube and the phosphine was added at defined time intervals using a precision syringe.

General Procedure for the Hydrogenation of 1-Hexene. (a) *P* = 1 bar. Toluene and 1-hexene were previously freeze−pump−thawed three times under H_2. To a Schlenk flask was added 5.21 × 10^{-3} mmol of rhodium complex and a magnetic stirring bar, and the system was evacuated and filled with H_2 three times. Toluene (6 mL) was added, and the system was stirred until dissolution of the solid. Meanwhile, the autoclave had been evacuated, filled with H_2, and fitted with hoses supplying water maintained at the desired temperature from the constant-temperature bath and the gas inlet had been connected to the H_2 line. Then 1-hexene (1 mL) was added to the Schlenk flask, the solution was rapidly transferred to the autoclave through the sample inlet via syringe, the gas inlet was opened, and the system was pressurized to 1 bar of H_2. The magnetic stirring was started and the timing counter reset. From the addition of the alkene to the reset of the timing counter no more than 3 min passed. After 1 h, the autoclave was vented and dismantled, and the composition of the solution was analyzed by capillary GC.

(b) *P* = 45 bar. The procedure used was as for P = 1 bar, but the reaction solutions and the autoclave were evacuated and filled three times with N_2 instead of H_2: rhodium complex, 5.21 × 10^{-3} mmol; 1-hexene, 5 mL; THF, 5 mL; 1 h.

Hydrogenation of Methacycline. The procedure used was as for the hydrogenation of 1-hexene at P = 45 bar: rhodium complex, 5.21 × 10^{-3} mmol; methacycline, 62.5 mg; MeOH−toluene (2:1), 6 mL; T = 75 °C; P = 45 bar; 7 h. The reaction mixture was analyzed by HPLC using a Macherey-Nagel column (ET 125-8-4 Nucleosil 100−5 C18 AB). The mobile phase was a mixture of 500 mL of 0.1 M sodium phosphate buffer containing 0.01 M EDTA, 500 mL of methanol, and 6 mL of *N*,*N*-dimethyloctylamine adjusted to pH 8 with 20% aqueous NaOH: flow rate, 1 mL min^{-1}; wavelength, 280 nm. The chromatographic peaks of methacycline, doxycycline, and *epi*-doxycycline were determined using authentic samples.

X-ray Structure Determination of [Rh(nH*PPh*)(PPh_3)$_2$]·3CH_2Cl_2. Single-crystal data collection was performed at ambient temperature on a Rigaku AFC5S diffractometer using graphite-monochromatized Mo Kα radiation. A total of 10 940 reflections giving 10 156 unique reflections (R_{int} = 0.036) were collected by the $\theta/2\theta$ scan mode ($2\theta_{max}$ = 50°).

Of those, 6323 were considered as observed according to the criterion $F > 4\sigma(F)$. Crystallographic data are presented in Table 2.

The structure was solved by direct methods using the MITHRIL program,[28] and the structure was refined on F by the XTAL3.2 program system.[29] Non-hydrogen atoms were refined with anisotropic displacement parameters in the final refinements. Positional parameters for the hydrogen atoms of the carborane cage were refined, but the rest of the hydrogen atoms were placed at their calculated positions. The final R value was 0.064 ($R_w = 0.068$).

(28) Gilmore, C. J. *J. Appl. Crystallogr.* **1982**, *17*, 42.
(29) Hall, S. R., Flack, H. D., Stewart, J. M., Eds. *Xtal3.2 User's Guide*; Universities of Western Australia, and Maryland, 1992.

Acknowledgment. This work was partially supported by the CIRIT under Project No. QFN95-4721 and the DGICYT under Project No. PB94-0226.

Supporting Information Available: A figure giving the full atom-numbering scheme and tables giving experimental details of the X-ray crystallographic analysis, atomic positional and isotropic displacements, atomic anisotropic displacements, and interatomic distances and angles for [Rh(nH*PPh*)-$(PPh_3)_2$]·CH_2Cl_2 (11 pages). Ordering information is given on any current masthead page.

OM971019M